PHYSICAL REVIEW A VOLUME 4, NUMBER 5 NOVEMBER 1971

Helium Ions at 76 °K: Their Transport and Formation Properties*

R. A. Gerber and M. A. Gusinow
Sandia Laboratories, Albuquerque, New Mexico 87115
(Received 5 April 1971)

The time dependences of the ion wall currents in a 76 °K helium afterglow were measured with a quadrupole mass-filter system. The species observed were He^+, He_2^+, He_3^+, He_4^+, and metastable atoms. The results of the present work are a zero-field mobility, $\mu_0(He^+)$, of $14.4 \pm 0.3\,cm^2 V^{-1} sec^{-1}$, and a three-body conversion frequency of He^+ into He_2^+ of $(1.44 \pm 0.14) \times 10^{-31} \times N^2\,sec^{-1}$, where N is the density in atoms/cm^3. The diffusion coefficient that describes the late-time behavior of He_3^+ was found to be $95.3 \pm 8.6\,cm^2\,sec^{-1}$ Torr. The metastable helium atoms at 76 °K were found to have a diffusion coefficient given by $D_m p_0 = 146\,cm^2\,sec^{-1}$ Torr. Evidence is presented for the presence of helium negative ions in the 76 °K helium afterglow.

INTRODUCTION

In the field of gaseous electronics the gas that has been most extensively studied is helium. This has occurred because it was quite naturally assumed, at least initially, that no ion complexes would form. However, it has been known for some time that He_2^+ is formed quite readily. Recently He_3^+ and He_4^+ have been shown to exist in 300 °K helium afterglow plasmas.[1]

The prime intent of this work is the study of helium molecular complexes and, in particular, their formation and transport properties. It is therefore most expedient to investigate a low-temperature (76 °K) helium afterglow, where formation of He_3^+ and He_4^+ is faster than at 300 °K. In particular, the species observed at 76 °K are He^+, He_2^+, He_3^+, He_4^+, and metastable atoms. The time behavior of the ion wall current as measured with a quadrupole mass filter leads us to conclude that the helium negative ion (He^- and/or He_2^-) is present in the afterglow.

EXPERIMENTAL APPARATUS AND TECHNIQUES

The vacuum system was constructed of stainless steel and glass. All valves were of the high-vacuum bakeable type. The entire system was baked at 300 °K for 24 h in order to obtain a base vacuum of 10^{-9} Torr.

The discharge tube (not to scale) is shown in Fig. 1. After bakeout and upon admitting cataphoretically pure helium, impurities (C^+, O^+, and CO^+) were observed in the afterglow. To rectify this problem it was found necessary to run a dc discharge (100 mA at 5 Torr initially) while pumping through the mass-filter aperture. Eventually the discharge extinguished itself at which time the remaining helium was pumped out. This was done from three to five times. The resultant sputtering of cathode material coated the glass walls in the vicinity of the cathode, thus covering up most of the impurities. The final cleanup was done by running a pulsed discharge for about 8 h at 5 Torr (300 °K). Upon completion of this cleanup procedure no impurity ions were observed. Tungsten, tantalum, nickel, and molybdenum were each used as electrode materials. It is important to mention that an acceptable impurity level was obtained only with molybdenum electrodes. The characteristic diffusion length Λ of the discharge tube was 0.178 cm. The sampling aperture was a 50-μ-diam hole in 25-μ-thick nickel sheet.

The mass analysis was performed with a quadrupole mass filter which operated at 4.7 MHz. The rods were 5 cm long with an r_0 of 0.25 cm. A schematic of the mass-filter arrangement and output counting circuitry is shown in Fig. 2. The mass filter was differentially pumped. Two different types of ion detectors were used. The first was a 14-stage Cu-Be dynode multiplier. This had a relatively low gain, and consequently it was difficult to count ions very late into the afterglow. However, because of its high saturation current limitation and relative insensitivity to photons and metastable particles it was possible to count ions in the very early afterglow. The second detector was a continuous surface channel multiplier. This had a higher gain than the dynode structure, and consequently it was possible to observe the ion decay further into the afterglow. It was, however, very sensitive to photons and metastables, and hence there existed a "background" which had to be subtracted from the total signal registered on the counter. The background was obtained either by reversing the polarity of G_1, which was typically biased at 50–200 V, or by making the mass filter unstable to all ions. The high flux of metastables and photons at very early times saturated the channel multiplier so that with this detector the very early afterglow was inaccessible to observation.

It was typically possible to observe the decay of the dominant ion, He_3^+ at 76 °K, over 6–7 decades of ion current (using the channel multiplier). However, because of saturation of the multiplier (and counter) at early times it was necessary to mod-

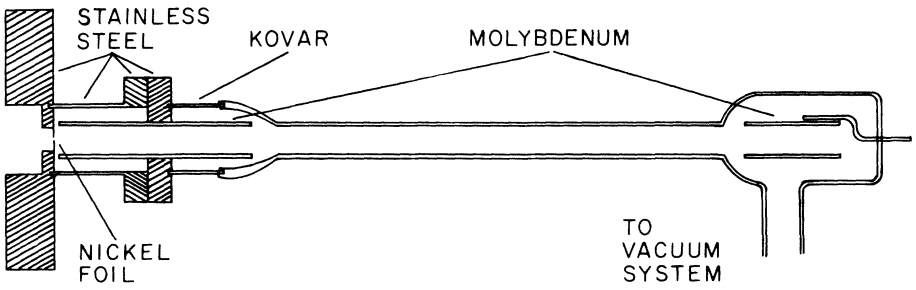

FIG. 1. The discharge tube and electrode assembly.

erate the ion current reaching the detector. This was effected by increasing the mass-filter resolution (by changing the ratio of the rf to dc potentials applied to the rods) in order to observe the early afterglow decay. The resulting decrease in transmission was done in three stages in order to fit together the entire afterglow decay. For the different resolutions no energy discrimination in the mass filter was observed. There was enough overlap between each of the three decay curves to ensure continuity.

RESULTS

The ions detected in the afterglow at a temperature of 76 °K were He^+, He_2^+, He_3^+, and He_4^+. Of these ions, He_4^+ was a minority ion at all gas pressures studied. In addition to the ion decay, the decay of the atomic metastables was obtained from the background signal. The pressure range of this study was from $p_0 = 0.7$ to 25 Torr, where p_0 is the pressure reduced to 273 °K, i.e., $p_0 = p(273\ °K/76\ °K)$. It is imperative to mention that all the measurements have been done with afterglows of ^3He, ^4He, and mixtures of the two. As a result of these isotope studies it is believed there were no impurity ion effects in the results presented here.

Typical afterglow measurements at two pressures are shown in Figs. 3 and 4. The decay curves for He_2^+ are not shown in these figures because these ions had the same time dependence as He^+. As shown in the figures He_3^+ was the dominant ion at late afterglow times. An analysis of the different ion species is given below.

He^+

At low pressures the majority of the observed He^+ ions were produced only during the discharge pulse. At higher pressure they were also produced during the afterglow period by atomic metastable collisions. The loss of the He^+ ions from the plasma at low pressures ($p_0 < 3$ Torr) is governed by diffusion to the walls and conversion to He_2^+ via the reaction

$$He^+ + 2He \rightarrow He_2^+ + He\ . \tag{1}$$

The late time dependence of He^+ under these conditions should be exponential and given by

$$[He^+] = [He^+]_0\, e^{-t/\tau}\ , \tag{2}$$

where

$$1/\tau = D_a/\Lambda^2 + Cp_0^2\ . \tag{3}$$

Here D_a is the electron-ion ambipolar diffusion coefficient of He^+ and $\nu_{conv} = Cp_0^2$ is the conversion frequency of process (1). It has been assumed here that diffusion and conversion are the only relevant loss processes. It has also been assumed that a fundamental diffusion mode distribution exists, where Λ is the characteristic diffusion length for this mode.

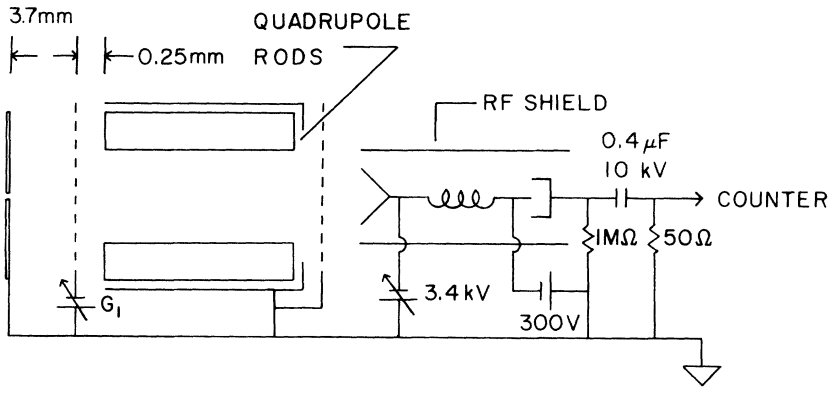

FIG. 2. The output counting circuitry and pertinent dimensions of the sampling system.

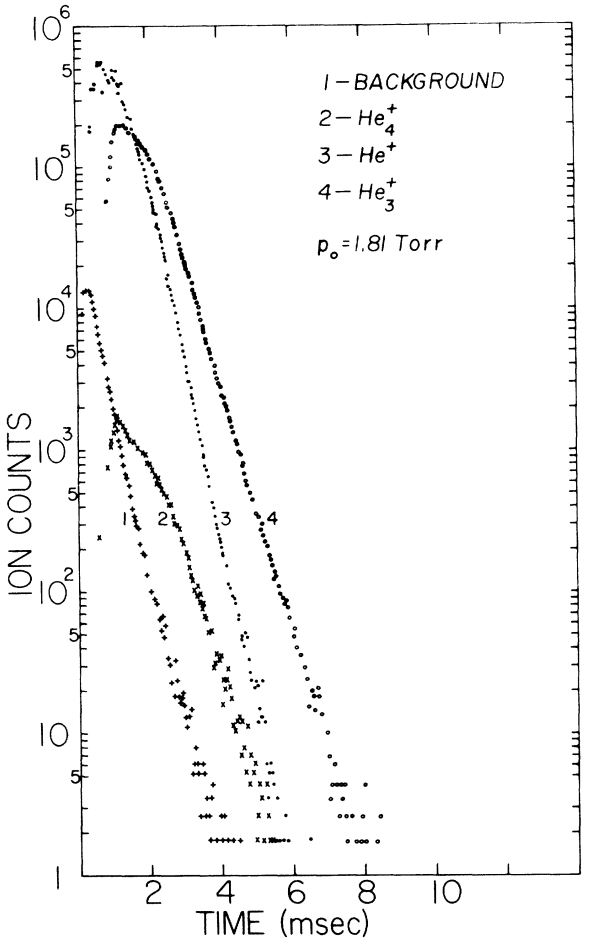

FIG. 3. The afterglow decay curves for the background, He_4^+, He^+, and He_3^+, at a reduced pressure of 1.81 Torr.

Since $D_a p_0$ is a constant, at a given temperature, a plot of p_0/τ vs p_0^3 should be linear. The intercept at zero pressure gives the quantity $D_a p_0/\Lambda^2$ while the slope gives the conversion constant C. Figure 5 shows the experimental plot of p_0/τ vs p_0^3. The intercept gives a value for the diffusion coefficient $D_a p_0$ of $144 \pm 3(2.2\%)$ cm^2 Torr sec^{-1}. The zero-field mobility value obtained from the Einstein relation ($\mu/D = e/kT$) for He^+ in He at 76 °K is $\mu_0 = 14.4 \pm 0.3$ cm^2 V^{-1} sec^{-1}. The conversion frequency obtained from Fig. 5 is $\nu_{conv} = [180 \pm 18(9.7\%)]p_0^2$ sec^{-1} (p_0 in Torr) or (in terms of the density N in atoms/cm^3) $\nu_{conv} = (1.44 \pm 0.14) \times 10^{-31} N^2$ sec^{-1}. The errors given here and in Fig. 5 represent the standard deviation from a least-squares fit of the data to a straight line. The lowest pressure data ($p_0 = 0.7$ and 1.0 Torr) in Fig. 5 were consistently below the straight line. This may be indicative of diffusion cooling.

At high pressures, the number of He^+ produced during the discharge pulse decayed very rapidly because of process (1). However, as shown in Fig. 4, there was a significant amount of He^+ at $p_0 = 10.83$ Torr. The density of He^+ at high pressure is indicative of production by metastable-metastable reactions

$$He^m + He^m \rightarrow He^+ + e + He \ , \qquad (4)$$

and consequently the time decay of He^+ is governed by the decay of He^m. The experimental results of He^+ at high pressures ($p_0 > 3$ Torr) will be given in the discussion of the metastable atoms.

He_2^+

As was found by Patterson[2] the diatomic molecular ion is converted into the triatomic ion He_3^+ via the reaction

$$He_2^+ + 2He \rightarrow He_3^+ + He. \qquad (5)$$

This reaction is faster than process (1) as evidenced by the fact that He^+ and He_2^+ have the same time behavior in the afterglow at both high and low pressures. Drift tube studies[2] have shown process (5) and its inverse to be in equilibrium over a temper-

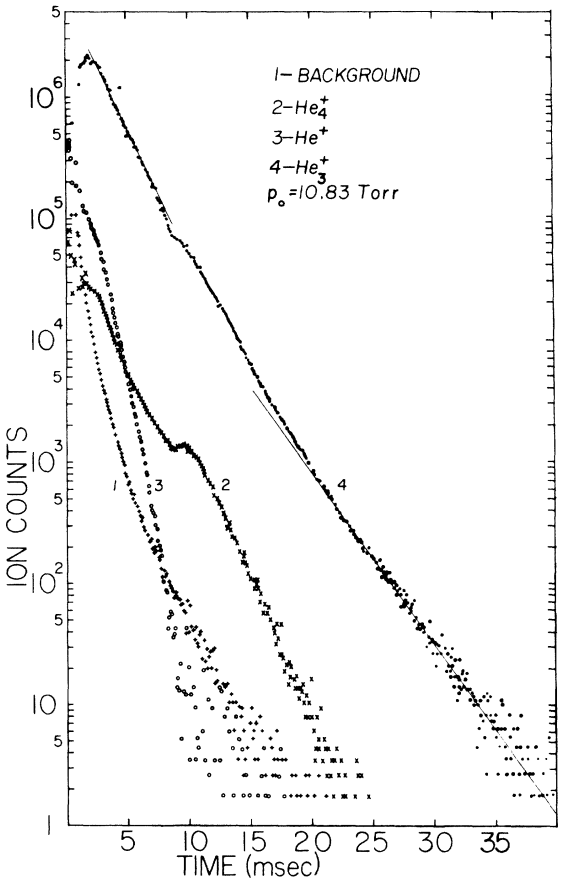

FIG. 4. The afterglow decay curves for the background, He^+, He_4^+, and He_3^+, at a reduced pressure of 10.83 Torr.

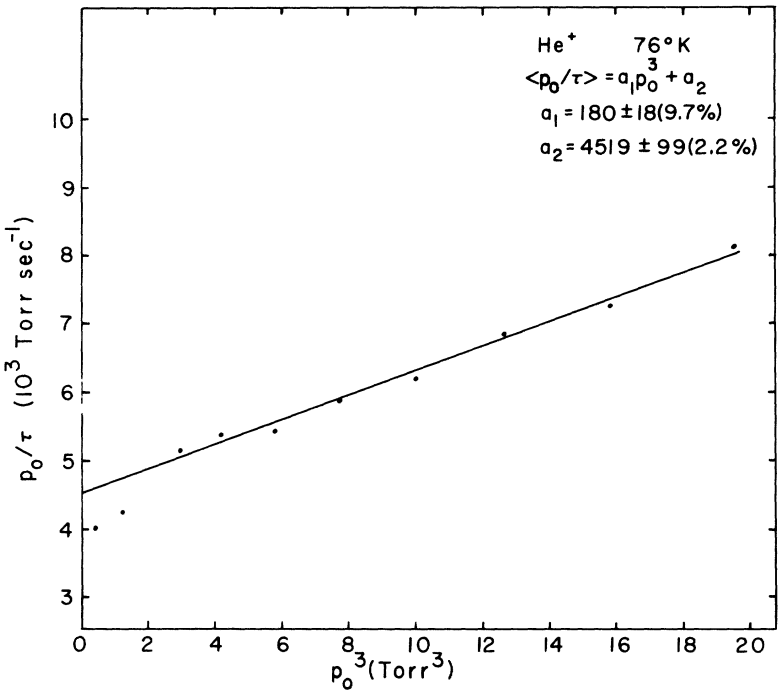

FIG. 5. The effective decay frequency of He^+ as a function of the reduced pressure cubed (p_0^3). The errors represent standard deviations derived from a least-squares fit of the data to a straight line.

ature range of 135 to 200 °K. He_2^+ and He_3^+ are in equilibrium at 300 °K as substantiated by afterglow measurements.[1] If He_2^+ and He_3^+ were in equilibrium at 76 °K, the number of He_2^+ relative to He_3^+, calculated from Ref. 2, would be $\sim 10^{-5}$. The measured ratio was greater than 10^{-5}, and the shapes of the decay curves were different. Therefore, He_2^+ and He_3^+ were not in equilibrium at 76 °K, presumably because the diatomic molecular ions were being produced by a combination of processes (1) and (4).

He_3^+

The triatomic ion He_3^+ was the dominant ion at late afterglow times as evidenced by Figs. 3 and 4.

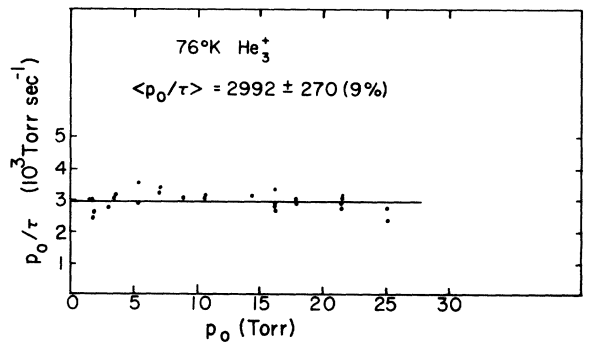

FIG. 6. The effective decay frequency of He_3^+ as a function of the reduced pressure (p_0). The error represents the standard deviation from the mean.

The late-time behavior of He_3^+ was exponential. A plot of p_0/τ vs p_0, where τ is the experimentally determined time constant, is shown in Fig. 6. The constancy of p_0/τ as a function of pressure shows that diffusion is the dominant loss process at late times. If the final decay is attributed to free diffusion, the data in Fig. 6 yield a value of (19.2 ± 1.7) $cm^2 V^{-1} sec^{-1}$ for the zero-field mobility of He_3^+ in helium at 76 °K. However, the behavior of He_3^+ leads us to believe that a helium negative ion is present during the afterglow period. The reasons are as follows:

(i) The range of the final experimental decay was, in many instances, measured over four or five orders of magnitude. The equipment used here had essentially the same sensitivity as that used to measure the transition from electron-ion ambipolar diffusion to free diffusion at 300 °K.[3] In the latter study it was found that the final free decay was at most over two orders of magnitude. It can be shown that the self-field of the ions [for $n_- = 0$, $E = (e/\epsilon_0 r) \int_0^r n_+ r\, dr$ in a cylindrical geometry] will prevent an exponential time decay if $n_+ \gtrsim 10^4$ cm^{-3}.

(ii) To clarify the following discussion Fig. 7 has been constructed to illustrate the general features of the transition out of electron – positive-ion ambipolar diffusion with and without negative ions. Figure 7 is a "schematic" picture based on both theory and experiment.[3-5] It has been assumed in constructing this picture that the diffusion coefficient of the negative ions is approximately equal to that of the dominant positive ions. The exact shapes

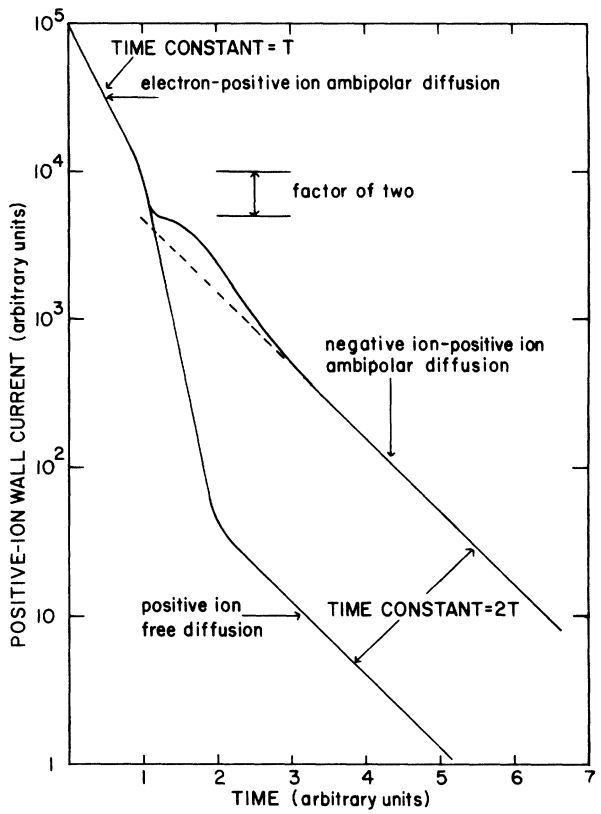

FIG. 7. A schematic picture illustrating the transition from electron–positive-ion ambipolar diffusion with and without negative ions. It has been assumed that the diffusion coefficient of the negative ion is approximately equal to that of the positive ion.

of the curves depends on the container size, the diffusion coefficients of the positive and negative ions, the formation and destruction rates of the negative ions, recombination of negative and positive particles, and the effect of there being more than one type of positive ion present.

The time dependence of the He_3^+ ion wall current has the same general features as the dominant ion wall current when negative ions are present.[4] The characteristics of a decay with negative ions present are (a) a region of electron-ion ambipolar diffusion, (b) a fast transition (to negative-ion – positive-ion ambipolar diffusion) which results in a sudden drop of the wall current by approximately a factor of 2 (if the diffusion coefficient of the negative ion D_- is approximately equal to that of the dominant positive ion D_+), and (c) an increase (or at least a tendency to increase) in the wall current following the transition. This increase has been ascribed to a redistribution of the density to a fundamental diffusion mode.[5]

The behavior of the He_3^+ ion current shown in Figs. 3 and 4 agrees with these predictions. (The transition in Fig. 4 occurs at approximately 8 msec.)

Within the scatter of the measurements p_0/τ could be attributed to free diffusion and/or positive-ion – negative-ion ambipolar diffusion, since D_a [$D_a = 2D_+D_-/(D_+ + D_-)$] would be approximately equal to D_+ if $D_- \approx D_+$. Clearly, the only conclusive proof for the existence of a helium negative ion in the 76 °K helium afterglow would be its detection with the mass filter. No negative ions were detected. It was necessary to apply an extraction voltage to G_1 to reduce space charge in the vicinity of the aperture to allow transmission of ions. Since He^- is only bound with 80 mV,[6] it is plausible that it was broken up because of collisions with the neutral gas in the neighborhood of the aperture.

It is important to note that the atomic helium negative ion has a finite lifetime[7] (it can spontaneously emit an electron). Consequently, when the plasma enters the negative-ion – positive-ion ambipolar diffusion regime (the electrons have left the volume) there is no longer negative-ion formation and the latter decay via diffusion and spontaneous emission of an electron. As the negative ions break up, the detached electrons rapidly leave the volume and consequently a large volume electric field develops due to the "excess" positive space charge. This increased space charge field can account for all or part of the increased positive-ion wall current. (In Fig. 4 the He_4^+ wall current does increase while that of He_3^+ shows an inflection.) Whether a specific positive-ion wall current shows a maximum or inflection depends in a rather critical fashion on the rate equations.

He_4^+

The He_4^+ ion is present in the helium afterglow at both room temperature[1] and at 76 °K. The time behavior of this ion at a gas temperature of 76 °K is shown in Figs. 3 and 4. Because of the relatively small amounts of He_4^+ and the fact that the transition occurs early in time, the diffusion coefficient could not be measured. It is not clear at this time how He_4^+ is produced. If it is produced by the reaction $He_3^+ + 2\,He \rightarrow He_4^+ + He$, then the conversion frequency for this reaction must be less than $1.5 \times 10^{-35} N^2$ sec^{-1}. This higher limit was obtained from Fig. 6, which shows that the maximum contribution from the latter process for the highest pressure used ($p = 25$ Torr) would be at most the uncertainty in the average value of p_0/τ.

As previously indicated, it was not possible under the conditions of the present work to make any quantitative measurements concerning He_4^+. However, it is necessary to discuss certain experimental observations and to make some speculations concerning this ion.

Just before the transition out of electron-ion

ambipolar diffusion at 76 °K and (in some work performed as a supplement to this experiment) at 300 °K there was a very small range of He_4^+ current that consistently indicated that the zero-field mobility of He_4^+ is approximately that of He^+. The range was too small to place any reliance on an estimate of the actual value.

At the early times in the 76 °K afterglow the He_4^+ wall current decayed rapidly and nonexponentially. This behavior can be indicative of recombination.[8] Since He_4^+ was a minority ion, it is not clear exactly what type of behavior is to be expected.

As inferred from the measured ion wall currents, the ratio He_4^+/He_3^+ is less at 76 °K than at 300 °K. This may be due to the fact that at 300 °K under the conditions of the experiment in Ref. 1 the dominant loss mechanism was diffusion. In this work the dominant ion loss at early times, at least for He_4^+, appears to have been recombination. It is also possible that the above ratio is less at 76 °K than at 300 °K because of an activation energy in some stage of the kinetics of the He_4^+ formation. This effect is, for example, known to occur in the formation of $He_2(^3\Sigma_u^+)$.[9]

ATOMIC METASTABLE ATOMS

The curve labeled background, shown in Figs. 3 and 4, was obtained when the mass spectrometer was made unstable to charged particles. At 300 °K this wall current at late times was shown to be proportional to the density of the molecular metastables.[10] At 76 °K we propose that the final decay is due to atomic metastables. This proposal is based in part on the work of Ref. 9. The decay of this background is exponential at late times. A plot of p_0/τ vs p_0 is shown in Fig. 8. The value obtained for $D_m p_0$ is 146 cm^2 sec^{-1} Torr, where D_m is the diffusion coefficient of the atomic metastables.

At high pressures ($p_0 > 3$ Torr) the time dependence of He^+ is governed by metastable-metastable collisions [process (4)]. If the dominant loss rate of He^m is by diffusion, then, since the diffusion loss of He^m is much slower than the conversion of He^+ into He_2^+, He^+ decays exponentially with a time constant given by $\tau = \Lambda^2/2D_m$. A few data points obtained from the decay of He^+ are shown in Fig. 8. The agreement between the two measurements indicates that process (4) is important at 76 °K and that the final experimental decay of the background is due to the atomic metastable atoms.

DISCUSSION

The zero-field mobility of He^+ at 76 °K obtained from this study is $\mu_0 = 14.4 \pm 0.3$ cm^2 V^{-1} sec^{-1}. This value is considerably lower than the value of 16.2 ± 0.3 obtained by Patterson[11] from drift tube studies. The present results are in fair agreement with the value of 13.5 obtained by Chanin and Biondi.[12] The three-body conversion frequency of He^+ into He_2^+ was found to be $(1.44 \pm 0.14) \times 10^{-31} N^2$ sec^{-1}. The value of $(1.7 \pm 0.4) \times 10^{-31} N^2$ sec^{-1} obtained in Ref. 2 overlaps that obtained here. If one uses the value of the conversion coefficient obtained by Phelps[13] at 300 °K and the value obtained here for 76 °K the temperature dependence can be estimated to be $\sim T^{-0.6}$. The temperature dependence calculated by Smirnov[14] was $T^{-0.75}$.

The coefficient describing the diffusion of He_3^+ was found to be $Dp_0 = 95.3 \pm 8.6$ cm^2 sec^{-1} Torr. From these measurements it is not possible to distinguish between free diffusion and ion-ion ambipolar diffusion. If the negative ion involved is He^-, then because of its relatively short lifetime ($\tau \sim 500$ μsec), the late-time decay, especially at high pressure, is free diffusion. The zero-field mobility obtained via the Einstein relation is 19.2 ± 1.7 cm^2 V^{-1} sec^{-1} which is in agreement with the value of 18.0 ± 0.3 cm^2 V^{-1} sec^{-1} from Ref. 11.

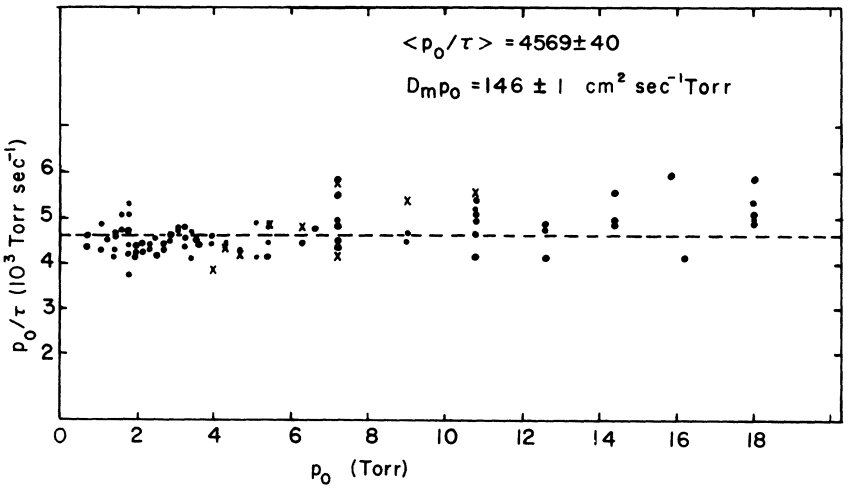

FIG. 8. The effective decay frequency of the helium atomic metastables as a function of the reduced pressure (p_0). The error represents the standard deviation from the mean. The data indicated by ×'s are those obtained from the decay of He^+ as explained in the text.

The diffusion of the atomic metastable particles at 76 °K was found to be described by $D_m p_0 = 146$ cm^2 sec^{-1} Torr. This is to be compared with the value of (163 ± 8) cm^2 sec^{-1} Torr of Ref. 15, which was obtained by using a diffusion cross section of 46×10^{-16} cm^2 ($\pm 5\%$) and Eq. (1) of that work.

The molecular ion He_2^+ was observed to have the same time dependence as He^+. This implies that the conversion of He_2^+ into He_3^+ is much faster than the conversion of He^+ into He_2^+. This finding is consistent with the results of Ref. 2.

The complete behavior of the positive-ion wall currents can be explained in a plausible fashion if one assumes the presence of negative helium ions in the afterglow. On the basis of Ref. 6, the atomic structure of He^-, and the presence of atomic metastable atoms in this work it is likely that the formation of the negative ions involves the atomic and/or molecular metastable particles. No negative ions were detected with the mass filter in the 76 °K afterglow and consequently their presence must be considered as conjectural.

*Work supported by the U.S. Atomic Energy Commission.

[1]M. A. Gusinow, R. A. Gerber, and J. B. Gerardo, Phys. Rev. Letters 25, 1248 (1970).

[2]P. L. Patterson, J. Chem. Phys. 48, 3625 (1968).

[3]R. A. Gerber, M. A. Gusinow, and J. B. Gerardo, Phys. Rev. 3, 1703 (1971).

[4]W. C. Lineberger and L. J. Puckett, Phys. Rev. 186, 116 (1969).

[5]Mark D. Kregel, J. Appl. Phys. 41, 1978 (1970).

[6]B. Brehm, M. A. Gusinow, and J. Hall, Phys. Rev. Letters 19, 737 (1967).

[7]G. N. Estberg and R. W. LaBahn, Phys. Rev. Letters 24, 1265 (1970).

[8]R. A. Gerber, M. A. Gusinow, and J. F. Freeman, Sandia Laboratories Report No. SC-RR-710089 (unpublished).

[9]A. V. Phelps and J. P. Molnar, Phys. Rev. 89, 1202 (1953).

[10]M. A. Gusinow and R. A. Gerber, Phys. Rev. A 2, 1973 (1970).

[11]P. L. Patterson, Phys. Rev. A 2, 1154 (1970).

[12]L. M. Chanin and M. A. Biondi, Phys. Rev. 106, 473 (1957).

[13]A. V. Phelps and S. C. Brown, Phys. Rev. 86, 102 (1952).

[14]B. M. Smirnov, Zh. Eksperim. i Teor. Fiz. 51, 1747 (1966) [Sov. Phys. JETP 24, 1180 (1967)].

[15]W. A. Fitzsimmons, N. F. Lane, and G. K. Walters, Phys. Rev. 174, 193 (1968).

PHYSICAL REVIEW A VOLUME 4, NUMBER 5 NOVEMBER 1971

Intensity-Correlation Spectroscopy*

V. Degiorgio† and J. B. Lastovka‡
Department of Physics and Center for Materials Science and Engineering, Massachusetts Institute of Technology, Cambridge, Massachusetts 02139
(Received 25 March 1971)

In recent years the utilization of "optical mixing" spectroscopic techniques in laser light scattering experiments has proved to be a successful method for the investigation of the dynamical properties of physical systems. By illuminating a photosensitive detector with the scattered light and measuring the spectrum or autocorrelation function of the resulting photocurrent, one can, in general, obtain the ensemble-average time dependence of specific collective excitations within the scattering medium. We present here a detailed quantitative analysis of the statistical errors inherent in such measurements due to the stochastic nature of both the scattering and photoemission processes. We determine the statistical errors on the optical-intensity correlation function as measured by two photocounting digital correlator models and on the intensity spectrum as measured by a "self-beat" optical mixing spectrometer. From these errors and a generalized least-mean-squares fitting procedure we calculate the uncertainty on the measured correlation time (linewidth) for the case of a Gaussian optical field with an exponential intensity correlation function (a Lorentzian spectrum). Scaling relationships are given which permit our numerical results to be applied to an arbitrary set of experimental parameters.

I. INTRODUCTION

In recent years the utilization of "optical mixing" spectroscopic techniques[1,2] in laser light scattering experiments has proved to be a successful method for the investigation of the dynamical properties of physical systems.[3,4] Very generally, the existence of scattering can be attributed to the presence of thermally excited collective and single-particle motions within the scattering medium.[5] Those normal modes of motion which are coupled to the optical dielectric susceptibility of the medium result in index-of-refraction inhomogeneities that are the source of the scattering. By considering the dy-